Article citation info:
Şirin G., Aydemir D., Gündüz G., Yörür H. 2024. Three-Dimensional Elastic Behavior of Oriental Plane (*Platanus orientalis* L.) Wood and Investigation Via Finite Element Analysis. *Drewno. Prace naukowe. Doniesienia. Komunikaty* 67 (213): 00027. https://doi.org/10.53502/wood-192553

Łukasiewicz Poznań Institute of Technology

Drewno. Prace naukowe. Doniesienia. Komunikaty
Wood. Research papers. Reports. Announcements

Journal website: https://drewno-wood.pl/

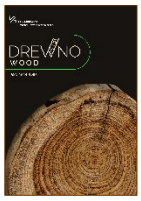

Three-Dimensional Elastic Behavior of Oriental Plane (*Platanus orientalis* L.) Wood and Investigation Via Finite Element Analysis

Göksu Şirin[a] *
Deniz Aydemir[b]
Gökhan Gündüz[c]
Hüseyin Yörür[d]

[a] Department of Forestry and Forest Products, Gaziosmanpaşa University, Almus Vocational School, Turkey
[b] Department of Forest Industry Engineering, Faculty of Forestry Bartın University, Turkey
[c] Department of Industrial Engineering, Faculty of Engineering and Natural Sciences, İskenderun Technical University, Turkey
[d] Department of Forest Engineering, Faculty of Forestry, Karabük University, Turkey

Article info
Received: 25 February 2022
Accepted: 12 August 2024
Published online:
27 August 2024

Keywords
experimental analysis
finite element analysis
mechanical properties
Oriental plane (*Platanus orientalis* L.)

Wood is an anisotropic material with a complex structure. It is very difficult to examine the properties of complex structured materials. Finite element analysis is a technique that can be used to analyze the mechanical behavior of wood and wood-based materials. The objective of this study is to determine the mechanical properties of Oriental plane (*Platanus orientalis* L.) wood both experimentally and using finite element analysis. For tensile strength and compressive strength, with the aim of determining the wood's behavior depending on its anisotropic axes, samples were prepared in three axial directions: radial, tangential and longitudinal. Under the same conditions and with the same dimensions, longitudinal samples were modeled in a computer environment using finite element analysis. ANSYS Multiphysics/LS-DYNA was used for simulation. It was determined that the laboratory results and the simulation results were in good agreement, with a similarity ratio of over 90%.

DOI: 10.53502/wood-192553

Introduction

Wood is a challenging material to describe [Ostapska and Malo 2020]. As a naturally grown material, wood has a sophisticated hierarchical structure and random defects and heterogeneities [Ostapska and Malo 2021]. Its unique physical properties are based on the structure of its cells and how they are arranged [Fu et al. 2023]. In order to determine the range of potential uses of a type of wood, the mechanical properties of the material must be determined. The mechanical properties of wood can be measured in experiments carried out at the sites where it is used, but they are usually determined by laboratory experiments. It is useful to investigate the relationships between wood and its mechanical responses to external

* Corresponding author: goksu.sirin@gop.edu.tr

influences in a number of ways. For example, for safety reasons (when wood failure has to be assessed), or in biomimetic-biomechanics (the development of new technical materials that mimic natural structures), having sufficient knowledge about the wood material will provide an advantage. This knowledge is also of great theoretical value. Although mechanical research on wood has a long history, many basic relationships are still unknown [Keunecke 2008]. Wood material has orthotropic properties and its axes are defined in three anatomical directions: longitudinal (parallel to the direction of the fiber or grain), radial (from the core to the bark), and tangential (parallel to the annual rings). The orthotropic character of wood affects almost all of its properties, including mechanical properties. This means that the elastic and strength properties of wood depend on its axial direction [Ożyhar 2013]. The material can therefore be understood completely and accurately only via examination in all three axes.

Today, rapid virtual analyses have begun to be carried out relating to the prevention or reduction of material loss, along with long-term time-saving experiments carried out in a computer environment, i.e., using numerical methods. These studies also allow the materials to be tested at the same time in many forms different from the original, and provide the opportunity to carry out biomechanical studies. Numerical methods can provide not only details of the material deformation process, but also information on changes in mechanical parameters during loading [Zhong et al. 2021]. Numerical methods are techniques in which problems are formulated mathematically so that they can be solved by arithmetic operations. In recent years, with the development of fast and efficient digital computers, numerical methods have played an important role in the solution of engineering problems. Numerical methods have the potential to solve a large number of equation systems, deviations from linearity, and complex geometries that are not at all uncommon in engineering applications and often cannot be solved by analytical methods [Arslantürk and Kara 2012]. Modeling with the finite element method is one of the techniques found in such studies [Warguła et al. 2020]. This is a numeric analysis method in which the problem is simulated while considering the physical conditions and features of the materials [Yörür 2012]. Finite element analysis allows a substance or material to be examined by dividing it into a very small finite number of elements to be analyzed. Even at these small size levels, changes can be monitored. Thus, the finite element method can provide a full solution where complex problems are divided into simpler sub-problems, with each one being solved within itself [Gürer et al. 2008]. For this purpose, the method uses three-dimensional models which are prepared or transferred to the computer environment. The accuracy of the results is proportional to the accuracy of the information transferred to the computer. The graphs obtained can be read and analyzed easily [Alhijazi et al. 2020]. Data obtained from experimental studies are necessary to create more accurate and effective numerical analyses.

Researchers deal with the experimental and numerical determination of material properties [Fajdiga et al. 2019] and have successfully applied this method in analyzing the properties of wood-based materials [Tabiei and Wu 2000; Moses 2004; Serrano 2004; Sheng et al. 2012]. It has been shown in many studies that the results of experiments and analyses concerning the mechanics of solid wood exhibit good agreement. However, when studies close to the present day are considered, it can be said that there is not enough research with the finite element method on wood and wooden materials. Güntekin and Yılmaz [2013] carried out analyses of the bending stresses and deformation of wooden beams. Wang and Lee [2014] investigated the feasibility of design and analysis of an interference fit in a dowel-glued joint by the finite element method. A predictive finite element model for laminated timber and laminated beams was developed by El Houjeyri et al. [2021]. This model was validated by comparison with experimental results. Toson et al. [2014] proposed a constitutive model for finite element modeling of balsa wood structures under severe loadings. Timbolmas et al. [2022] used the finite element method to analyze the behavior of poplar wood subjected to axial tensile stress. Hajdarević and Busuladžić [2015] presented a stiffness analysis of a statically indeterminate wooden chair side-frame. They reported good agreement between the results of numerical analysis and those of experimental testing of wood specimens. Dos Santos et al. [2015] proposed non-linear 3D finite element models to simulate T-joint behavior. In another study, the mechanical behavior of notched wood beams was studied using full-field measurements and modeled using finite element software [Toussaint et al., 2016]. Pěnčík [2015] conducted research on the modeling of experimental tests of wooden specimens from Scots pine. Hu et al. [2019] studied the effect of size on the mechanical properties of European beech wood, using samples of different sizes. Meghlat et al. [2013] developed a new approach to model nailed and screwed timber joints using the finite element method. Fajdiga et al. [2019] studied computational and experimental results on the fracture behavior of spruce wood under quasi-static loading conditions during a three-point bending test. Kaygın et al. [2016] determined the strength properties of wood corner joints using finite

element analysis, and obtained agreement at a level of about 90–97%. Zulkifli et al. [2021] performed numerical simulation of the behavior of wood materials under high strain rates using finite element software. They reported that the results differed from the experimental results by not more than 10%.

The main purpose of the present study was to examine the properties of wood samples in the tangential, radial and longitudinal axes using tensile and compressive strength tests, and to repeat the experiments in the same form in a computer environment. Thus, the aim was to determine the possibility of using finite element analysis instead of physical tests on solid wood. To accomplish this aim, the following operations were performed:

1. In a laboratory environment, mechanical experiments were conducted using *Platanus orientalis* L. trunk wood samples oriented in three different directions (radial, tangential and longitudinal). At this stage, the aim was to observe the behavior of the wood in different axial directions and to determine the rupture parameters. The collected data set was used to determine the material properties necessary to construct the model used in finite element analysis of the samples.
2. Due to the natural growing process and growth direction, mechanical properties such as stiffness and strength are assumed to vary mainly in the longitudinal direction [Kandler et al. 2015]. Numerical simulations were performed for longitudinally directed specimens. Parallel-to-fiber tensile strength and compressive strength tests were repeated using finite element analysis, and the results were computed for models under the same loading conditions. At this stage, the aim was to see how close the results obtained by simulating a natural structure in a computer environment could be to those obtained under natural conditions.

Materials and methods

1. Test specimens

For the experimental determination of mechanical properties, Oriental plane (*Platanus orientalis* L.) wood was obtained from the Kozcağız district in the province of Bartın in northern Türkiye. All experiments were performed with samples from the same wood. Samples for compressive strength and two different types of tensile strength samples were prepared for the tests. Test samples were prepared after planks from Oriental plane were brought to 65% relative humidity and 12% equilibrium humidity at 20 °C. The DB-shaped samples and parallel-to-fiber tensile strength samples were prepared in a five-axis CNC machine. To obtain accurate results, the specimens were prepared in their final form for the tests by means of a one-month holding period in an acclimatization cabinet at 65% relative humidity and at 20 °C.

Dog-bone shaped samples (DB) were used to test the tensile strength characteristics of the neck form in particular. After their final shape was formed, the two end faces of the DB specimens were supported by beech wood pieces. This meant that the samples were not damaged during the experiments. The material used for experimental samples did not include knots, reaction wood or heartwood. Figure 1 shows the sample dimensions.

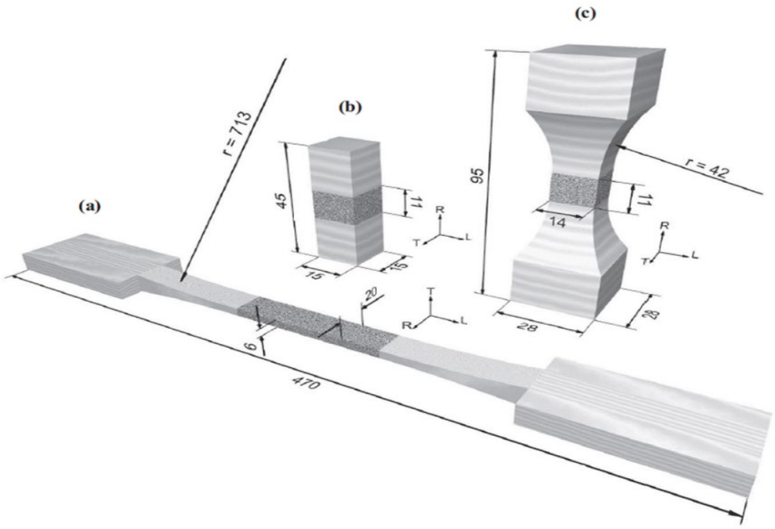

Fig. 1. Sample dimensions: (a) tensile strength parallel-to-fiber sample; (b) compressive strength sample; (c) DB-shaped samples (all dimensions in mm) [Ożyhar 2013]

2. Method

DB-tensile samples were prepared according to the DIN 52188 (1979) standard as 95 mm long with 20 × 20 mm ends and a middle section of 14 × 14 mm. The two end sides of the samples were supported with 4 mm thick and 26 mm long beech wood pieces. All experiments were carried out according to TSE (Turkish Standardization Institute) requirements and completed in 90 ± 30 seconds. Sixty samples were used for the experiments. The AG-IS Shumadzu 50 KN-powered universal test device was used for the DB-shaped sample tests. For the tests the speed of the test device was set as 5 mm/min for radial axis samples and 3 mm/min for tangential samples. Parallel-to-fiber tensile strength tests were carried out according to the TS 2475 standard. Sixty samples were used for the experiments. The Instron 60-ton universal tester was used for the parallel-to-fiber tensile tests. For the tests the machine speed was set at 4 mm/min. Similar test variables were used for both DB-tensile and parallel-to-fiber tensile testing. Modulus of elasticity was calculated using equation (1) in accordance with the relevant standards.

$$E_i = \frac{\Delta\sigma_i}{\Delta\varepsilon_i} = \frac{\sigma_{2i} - \sigma_{1i}}{\varepsilon_{2i} - \varepsilon_{1i}} \quad (1)$$

In this equation, E is the modulus of elasticity in withdrawal, $\Delta\sigma_i$ is the difference between the two compressive values, $\Delta\varepsilon_i$ is the difference between the two deformation values, and i is a variable representing tangential, radial and parallel-to-fiber axes.

For compressive strength, eighty samples were prepared in tangential, radial and longitudinal directions. The test was carried out according to DIN 52185 (1976) and DIN 52192 (1979). Samples were prepared with dimensions of 15 × 15 × 45 mm. Experiments were carried out according to TSE in 90 ± 30 seconds. The Utest 10-ton powered universal test device was used for the experiments, with the machine speed set at 2 mm/min. Equation (1) was also used to calculate the compressive strength modulus of elasticity.

The values obtained from the test results were transferred to the computer environment and the ANSYS program was used for finite element analysis. The finite element model required for calculation was created in the same processor. The finite element model data files created in a three-dimensional environment were transferred to the LS-DYNA and analyzed. Solid 164 was chosen as the material for modelling.

Results and discussion

1. Mechanical property findings

To determine the mechanical properties, tests were carried out after the radial, tangential and longitudinal compressive strength and tensile strength samples obtained from the trunk wood of the tree were brought to the appropriate humidity level. After completion of the experiments, the modulus of elasticity was calculated for each of the samples and the mean values were determined. The results were compared with the results of the finite element analysis. Due to its natural structure, *Platanus orientalis* L. contains a large amount of wide ray band. The sawdust formed from the tangential and radial axes samples contained large amounts of ray bands.

For the DB-shaped samples, the maximum force (F_{max}) and tensile strength (TS) values obtained according to the results of the experiments are given in Tables 1 and 2 below. In nearly all of the samples, rupture occurred in the middle of the sample, as expected.

Table 1. F_{max} values for dog-bone samples

Axis of specimen	N	(N)	S (±)	Max. (MPa)	Min. (MPa)
Tangential	60	1548.7	363.8	3050.0	695.3
Radial	60	2407.1	623.6	3696.9	1173.4

Table 2. TS values for dog-bone samples

Axis of specimen	N	(MPa)	S (±)	Max. (MPa)	Min. (MPa)
Tangential	60	7.9	1.3	10.9	5.5
Radial	60	12.2	3.0	18.9	6.1

From the tangential and radial measurements, it was observed that the radial samples exhibited higher resistance in tensile strength tests than the tangential samples. Table 3 shows the results of the LSD test for the tangential and radial axis samples.

For parallel-to-fiber tensile strength samples, the results obtained from the experiments are given in Table 4.

As was expected, the rupture occurred in the middle of all of the samples. The ruptured section was not very sharp, as in the case of the tangential and radial axis DB samples; however, in some samples it had been fragmented due to the effect of the fibers.

Figure 2 shows the relationship between tensile strength and density. According to these results, a high correlation was found between the tensile strength of the three axes and the density variation. The highest correlation was obtained for tensile strength in the radial axis (84%), and the lowest in the case of the tangential axis (73%).

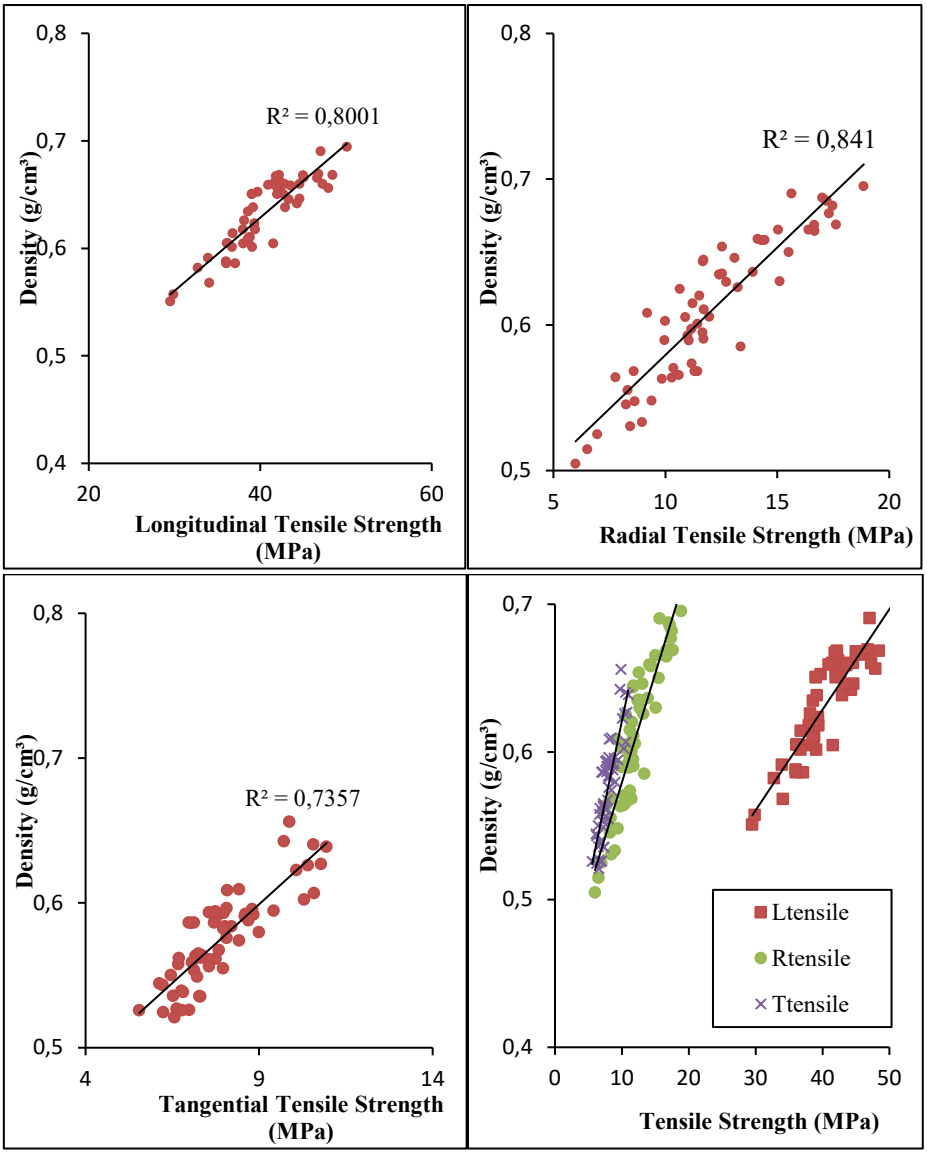

Fig. 2. Relationship between tensile strength values and density

Table 3. LSD test results for tangential and radial dog-bone samples

Axis of specimen	N	F_{max} (N)*	TS (MPa)*
Tangential	60	1548.7 A	7.9 A
Radial	60	2407.1 B	12.2 B

*$p < 0.05$

Table 4. TS values for parallel-to-fiber tensile strength specimens

Axis of specimen	N	(MPa)	S (±)	Max. (MPa)	Min. (MPa)
Tensile strength parallel to fibers	60	40.4	4.8	50.1	29.5

For compressive strength, the longitudinal specimens exhibited a bending behavior instead of sharp rupture. This behavior was seen at much lower rates in the tangential and radial samples. Due to its characteristic structure, plane tree wood exhibited bending behavior in some of the samples. This property of the wood is due to the large amount of wide rays that it contains, and also to its fiber structure. Therefore, when the experiment could not be conducted within the period defined by experimental standards, it was ended when 5% deformation of the sample size was reached. The tangential and radial axis samples were similar to each other in that they produced results in a shorter time than the longitudinal axis samples. F_{max} and compressive strength (CS) measurements obtained from the experiments are given in Tables 5 and 6.

According to the tangential, radial and longitudinal axis measurements, the highest resistance was obtained in the longitudinal specimens. The tangential and radial samples exhibited lower resistance. In Table 7, LSD test results are given for the tangential, radial and longitudinal axes.

Figure 3 shows the relationship between compressive strength and density. According to these results, a high correlation was found between the compressive strength of the three axes and the density variation. The highest correlation was obtained for tensile strength in the tangential axis (78%), and the lowest correlation in the case of the radial axis (73%).

The results for the modulus of elasticity of the specimens in the DB radial and tangential axes and tensile strength in the parallel-to-fiber axis are shown in Table 8. According to the data for the tangential and radial axes, the modulus of elasticity values were similar, while parallel-to-fiber samples gave higher values.

Table 5. F_{max} values for compressive strength samples

Axis of specimen	N	(N)	S (±)	Max. (MPa)	Min. (MPa)
Tangential	80	1303.06	231.85	2146	1008
Radial	80	1953.28	692.18	4785	1040
Longitudinal	80	8841.01	1153.37	11717	6966

Table 6. CS values for compressive strength samples

Axis of specimen	N	(MPa)	S (±)	Max. (MPa)	Min. (MPa)
Tangential	80	5.8	1	9.5	4.5
Radial	80	9	2.5	18.4	4.9
Longitudinal	80	38.9	4.4	52	31

Table 7. LSD test results for tangential, radial and longitudinal samples

Axis of specimen	N	F_{max}(N)*	CS (MPa)*
Tangential	80	1303.06A	5.8A
Radial	80	1953.28B	9B
Longitudinal	80	8841.01C	38.9C

*$p < 0.05$

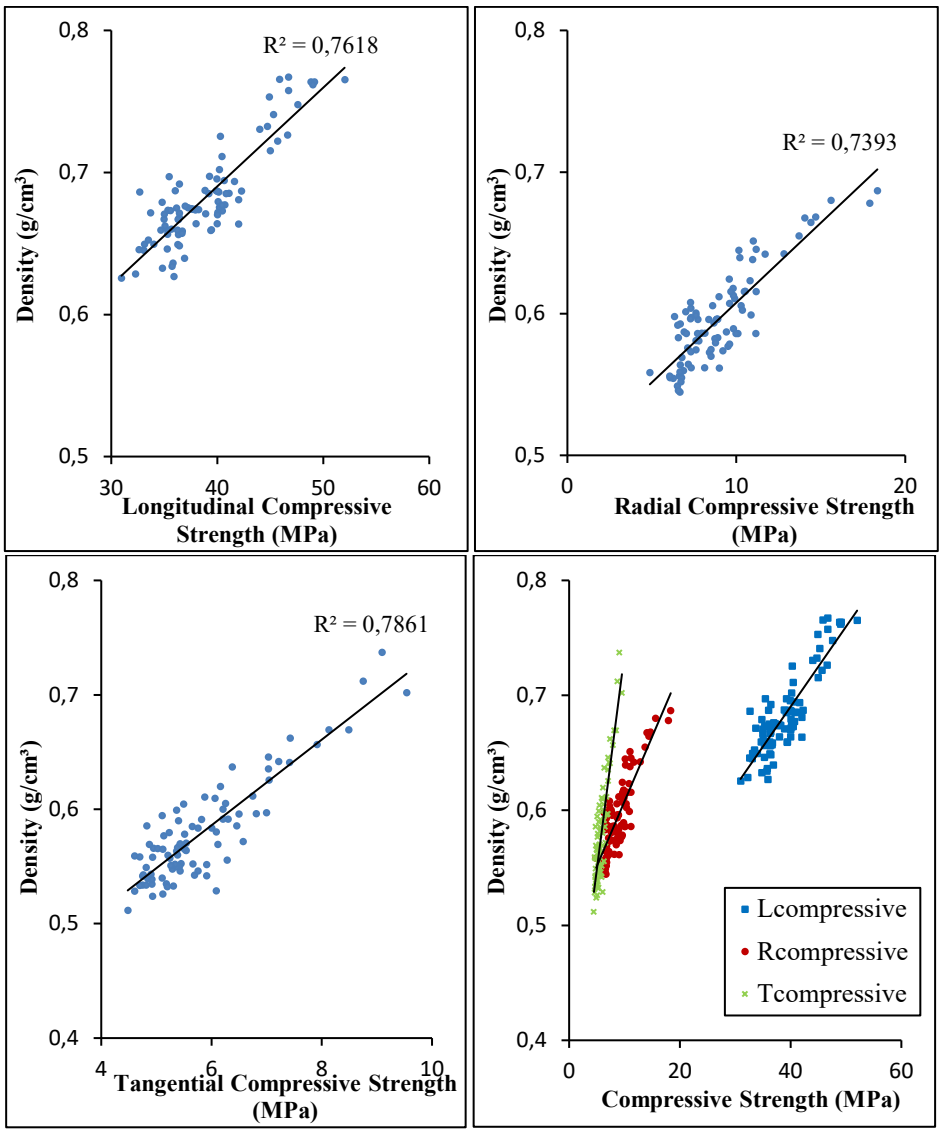

Fig. 3. Relationship between compressive strength values and density

Table 8. Modulus of elasticity results for test specimens for tensile strength parallel to fibers and DB tangential and radial axis

Axis of specimen	N	Modulus of elasticity
Longitudinal, parallel to fibers	60	4680.5
Tangential	60	388.9
Radial	60	559.2

According to the DB measurements, the longitudinal axis samples exhibited the highest resistance. The tangential and radial samples demonstrated lower resistance. Table 9 shows the LSD test results.

The modulus of elasticity results for the compressive strength samples are given in Table 10. The maximum compressive strength is in the longitudinal direction and the minimum in the tangential direction. Table 11 shows the LSD test results.

Table 9. LSD results for modulus of elasticity of tensile strength samples for parallel-to-fiber longitudinal and DB tangential and radial axes

Axis of specimen	N	TS modulus of elasticity (MPa)*
Longitudinal, parallel to fibers	60	4680.5 A
Tangential	60	388.9 B
Radial	60	559.2 B

*$p < 0.05$

Table 10. Modulus of elasticity results for test specimens for compressive strength in the tangential, radial and longitudinal axes

Axis of specimen	N	Modulus of elasticity
Longitudinal	80	7105.6
Tangential	80	354.3
Radial	80	761.2

Table 11. LSD results for modulus of elasticity for tangential, radial and longitudinal axis compressive strength samples

Axis of specimen	N	CS modulus of elasticity (MPa)*
Longitudinal	80	7105.6 A
Tangential	80	354.3 B
Radial	80	761.2 B

*$p < 0.05$

2. Finite element analysis results

In the study, after using *Platanus orientalis* L. samples for laboratory tests of tensile strength and compressive strength in the tangential, radial and longitudinal axes, finite element analysis was performed for parallel-to-fiber tensile strength and longitudinal compressive strength test samples. The samples were simulated in three dimensions using the ANSYS finite element program. After determining the necessary and appropriate information for the samples, analyses were performed using LS-DYNA. The data obtained under laboratory conditions were used for the analysis in the simulation environment. The data transferred to the ANSYS/LS-DYNA program yielded deformation and stress values for the samples. All three axial directions were created in the simulation environment. Analyses were conducted by selecting the longitudinal direction. Figures 4 and 5 show the simulation images obtained as a result of the parallel-to-fiber tensile strength and longitudinal compressive strength tests in the computer environment under the same conditions as those in the laboratory.

Figure 4 shows the stress distributions of tensile strength. The *x*-coordinate was chosen for the parallel-to-fiber tensile strength analysis in the simulation environment. The stress increased with the load, and it was found that the highest stress occurred in the middle sections where the ruptures had occurred. In the area where the stress is highest, the stress in the sample was observed with the help of Ls-prepost. Rupture occurred in the specimen after stress. In the analyses, it was determined that the stress decreased from these points to the edges of the sample. In the highest stress area, a measurement of 47.5 MPa was obtained. The value dropped after the rupture. In the analyses, it was seen that the results of the experiments under laboratory conditions and those of the computer environment were 90–98% compatible for the parallel-to-fiber tensile strength samples.

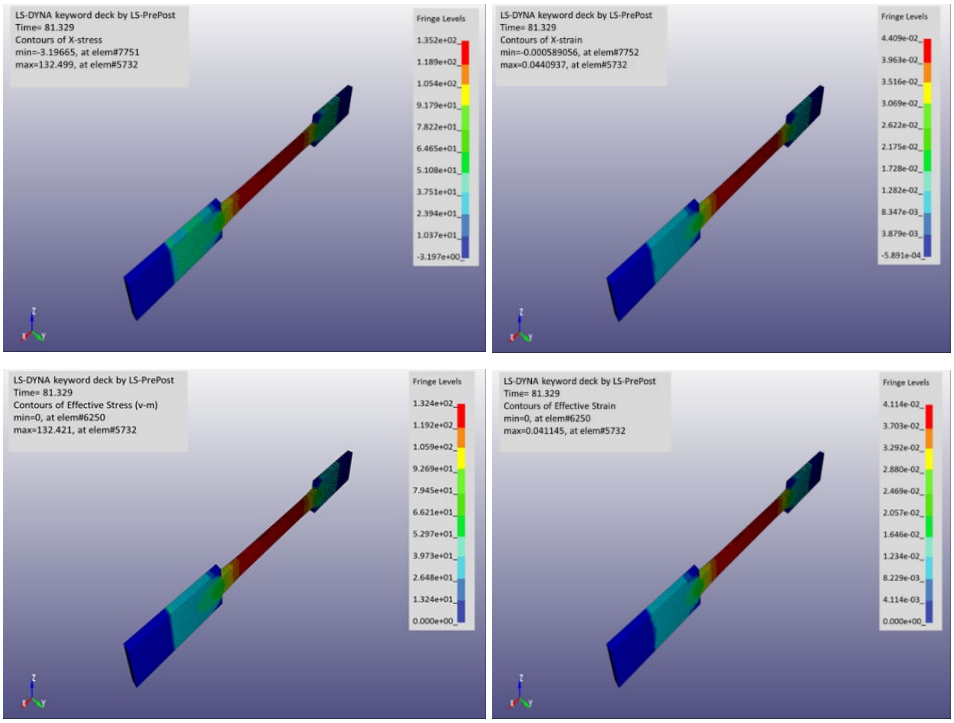

Fig. 4. Stress/deformation results for parallel-to-fiber tensile strength samples

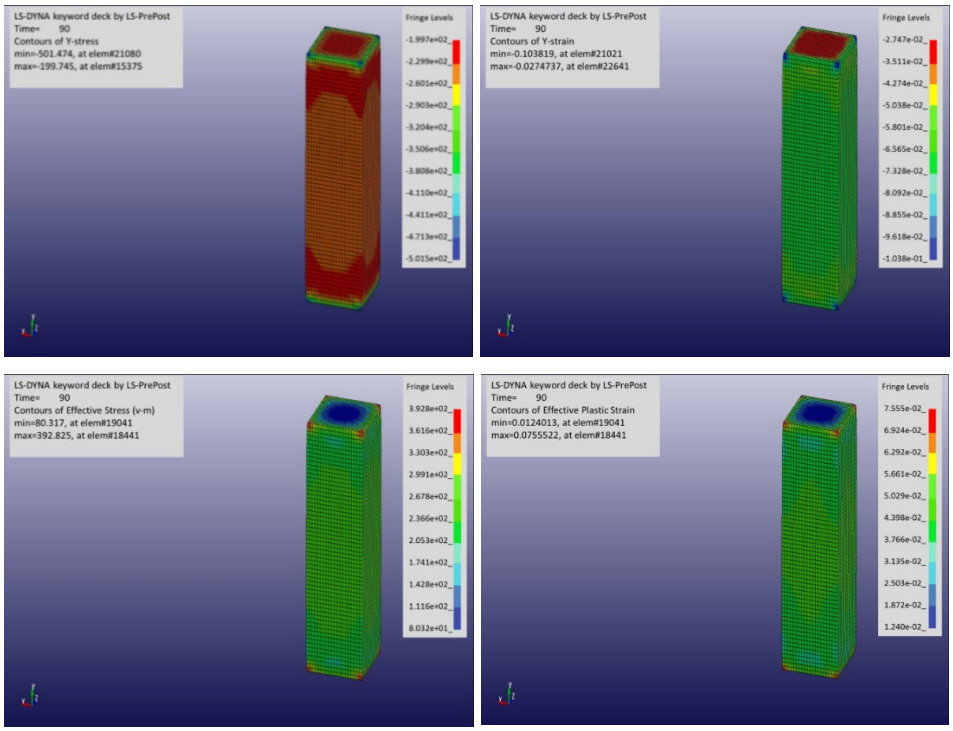

Fig. 5. Stress/deformation results for longitudinal axis compressive strength samples

Figure 5 shows the stress distributions in the compressive strength case. For the compressive strength analysis, the *y*-coordinate was chosen in the simulation environment. With the help of Ls-prepost, the stress in the sample was observed at the support and contact points where the force was applied. The stress increased with the load. The maximum stress value for the compression strength samples was 50.4 MPa. This value began to decline from the moment of rupture. In the analyses, it was seen that the results of the experiments under laboratory conditions and those of the computer analysis were 90–98% compatible for the compressive strength samples.

Table 12. Results of parallel-to-fiber tensile strength and longitudinal compressive strength tests obtained under laboratory conditions and via computer-aided analysis

Specimen	Experimental (MPa)	ANSYS/LS-DYNA (MPa)
Tensile strength parallel to fibers	50.1	47.5
Compressive strength, longitudinal	52	50.4

Hu et al. [2021] studied the mechanical properties of beech wood in compression and tension by experimental and numerical methods. It was reported that the results of the finite element model were all highly consistent with those measured by means of compression and tension experiments. Collins et al. [2023] constructed a numerical model to predict tensile strengths, and reported that it made the predictions successfully. In another study, simulated compressive curves for varying moisture contents and three grain directions were obtained by the finite element method, and were compared with curves obtained by experiment. It was reported that the trend seen in the results of the finite element analysis was consistent with the experiment in terms of the effects of moisture content and grain direction [Fu et al. 2021].

Table 12 shows the results obtained by testing and with the use of computer-aided analysis.

It is seen that the finite element models generated predict the values with relatively high accuracy.

The effectiveness of the simulations is evidenced by the comparison with the results of experimental tests. In the numerical analysis, the results are lower. This can be explained by the higher sensitivity of simulation analyses compared with experimental ones, and the anisotropy of wood materials.

Conclusions

In this study, *Platanus orientalis* L. trunk wood was investigated using various mechanical experiments and by the finite element method. The use of samples of "dog-bone" shape is important because of the varying properties of the wood according to the axial direction. Due to their size, it was possible to prepare these samples in the radial and tangential axial directions of the wood. In this way, more detailed information was obtained in smaller regions and for different directions of the anisotropic wood structure. Longitudinal tensile and compressive strength specimens were successfully simulated using the finite element method. The stress distribution was clearly visible in the simulation models. The results obtained from the experiments and from the numerical analysis were compared, and it was determined that there was a high degree of agreement. The research revealed that the finite element method used in the study provides a convenient method for determining the behavior of solid wood, and can be used in determination of the mechanical properties of Oriental plane wood.

The different behavior of wood in different axes, that is, its anisotropic structure, can create difficulties in analysis. However, this indicates a need to continue research on the development of the analyses performed and programs used. Finite element analysis is a powerful adjunct that has to be allied with experimental observation and material characterization [Vasic et al. 2005]. With the results of computer-aided analysis programs and modeling closely approximating those of experimental methods, it is predicted that finite element analysis methods will be used more effectively in the future.

Acknowledgements

This study was prepared by Göksu Şirin as a PhD thesis at the Department of Forest Industry Engineering, Faculty of Forestry, Bartın University. We would like to thank Bartın University and Karabük University for the experimental studies. This thesis was supported by the Scientific Research Projects Coordination Unit of Bartın University with the project number BAP-2013.1.91.

References

Alhijazi M., Zeeshan Q., Qin Z., Safaei B., Asmael M. [2020]: Finite element analysis of natural fibers composites: A review. Nanotechnology Reviews, 9 [1], 853-875. DOI:10.1515/ntrev-2020-0069

Arslantürk C., Kara Y. A. [2012]: Numerical methods lecture notes (in Turkish). Engineering Faculty, Atatürk University, Erzurum, Türkiye

Collins S., Jaaranen J., Fink G. [2023]: Modelling the effect of three-dimensional grain angle on the tension strength of birch wood. World Conference on Timber Engineering [pp. 428-434]. DOI: 10.52202/069179-0058

Dos Santos, C. L., Morais, J. J. L., De Jesus, A. M. P. [2015]: Mechanical behaviour of wood T-joints. Experimental and numerical investigation. Frattura ed Integrità Strutturale, 9 [31], 23-37. DOI: 10.3221/IGF-ESIS.31.03

El Houjeyri, I., Thi, V. D., Oudjene, M., Ottenhaus, L. M., Khelifa, M., Rogaume, Y. [2021]: Coupled nonlinear-damage finite element analysis and design of novel engineered wood products made of Oak hardwood. European Journal of Wood and Wood Products, 79, 29-47. DOI: 10.1007/s00107-020-01617-7

Fajdiga G., Rajh D., Nečemer B., Glodež S., Šraml M. [2019]: Experimental and numerical determination of the mechanical properties of spruce wood. Forests, 10 [12], 1140. DOI: 10.3390/f10121140

Fu Z., Chen J., Zhang Y., Xie F., Lu Y. [2023]: Review on wood deformation and cracking during moisture loss. Polymers, 15 [15], 3295. DOI:10.3390/polym15153295

Fu W. L., Guan H. Y., Kei S. [2021]: Effects of moisture content and grain direction on the elastic properties of beech wood based on experiment and finite element method. Forests, 12 [5], 610. DOI: 10.3390/f12050610

Güntekin E., Yılmaz T. [2013]: Eğilmeye çalışan budaklı kirişlerin sonlu elemanlar modelleri. SDU Faculty of Forestry Journal, 14, 53-7.

Gürer C., Akbulut H. Çetin, S. [2008]: Tek açıklıklı kemer sistemli Rize köprülerinin sonlu elemanlar yöntemi ile analizi (Analysis of single span arch system Rize bridges by finite element method). 1. Bridge and Viaducts Symposium. November 26-28. Antalya, Türkiye

Hajdarević S., Busuladžić I. [2015]: Stiffness analysis of wood chair frame. Procedia Engineering, 100, 746-755. DOI: 10.1016/j.proeng.2015.01.428

Hu W., Chen B., Zhang T. [2021]: Experimental and numerical studies on mechanical behaviors of beech wood under compressive and tensile states. Wood Research, 66, 27-38. DOI: 10.37763/wr.1336-4561/66.1.2738

Hu W., Wan H., Guan H. [2019]: Size effect on the elastic mechanical properties of beech and its application in finite element analysis of wood structures. Forests, 10 [9], 783. DOI: 10.3390/f10090783

Kandler G., Füssl J., Eberhardsteiner J. [2015]: Stochastic finite element approaches for wood-based products: theoretical framework and review of methods. Wood Science and Technology, 49, 1055-1097. DOI:10.1007/s00226-015-0737-5

Kaygın B. Yörür H. Uysal B. [2016]: Simulating strength behaviors of corner joints of wood constructions by using finite element method. Drvna Industrija, 67 [2], 133-140. DOI: 10.5552/drind.2016.1503

Keunecke D. [2008]: Elasto-mechanical characterizations of yew and spruce wood with regard to structure property relationships. PhD thesis, University of Hamburg, Germany. DOI: 10.3929/ethz-a-005629078

Meghlat E. M., Oudjene M., Ait-Aider H., Batoz J. L. [2013]: A new approach to model nailed and screwed timber joints using the finite element method. Construction and Building Materials, 41, 263-269. DOI: 10.1016/j.conbuildmat.2012.11.068

Moses D. M., Prion H.G.L. [2004]: Stress and failure analysis of wood composites: A new model. Composites: Part B: Engineering, 35: 251–261. DOI: 10.1016/j.compositesb.2003.10.002s

Ostapska K., Malo K. A. [2020]: Wedge splitting test of wood for fracture parameters estimation of Norway Spruce. Engineering Fracture Mechanics, 232, 107024. DOI:10.1016/j.engfracmech.2020.107024

Ostapska K., Malo K. A. [2021]: Crack path tracking using DIC and XFEM modelling of mixed-mode fracture in wood. Theoretical and Applied Fracture Mechanics, 112, 102896. DOI:10.1016/j.tafmec.2021.102896

Ożyhar T. [2013]: Moisture and time dependent orthotropic mechanical characterization of beech wood. PhD thesis. Technical University of Munich, Germany. DOI: 10.3929/ethz-a-009787740

Pěnčík J. [2015]: Modelling of Experimental Tests of Wooden Specimens from Scots Pine [Pinus sylvestris] with the Help of Anisotropic Plasticity Material Model. Wood Industry/Drvna Industrija, 66 [1]. DOI: 10.5552/drind.2015.1362

Serrano E. A. [2004]: Numerical study of the shear-strength-predicting capabilities of test specimens

for wood–adhesive bonds. International Journal of Adhesion & Adhesives, 24: 23-35. DOI: 10.1016/s0143-7496(03)00096-4

Sheng H., Feng F., Lan-Ying L., Ping-Xiang C. [2012]: Application of finite element analysis in properties test of finger-jointed lumber. Proceedings of the 55th International Convention of Society of Wood Science and Technology. August 27–31. Beijing, China

Tabiei A., Wu J. [2000]: Three-dimensional nonlinear orthotropic finite element material model for wood. Composite Structures, 50:143-149. DOI: 10.1016/s0263-8223(00)00089-1

Timbolmas C., Rescalvo F. J., Portela M., Bravo R. [2022]: Analysis of poplar timber finger joints by means of Digital Image Correlation [DIC] and finite element simulation subjected to tension loading. European Journal of Wood and Wood Products, 80 [3], 555-567. DOI: 10.1007/s00107-022-01806-6

Toson B., Viot P., Pesqué J. J. [2014]: Finite element modeling of Balsa wood structures under severe loadings. Engineering Structures, 70, 36-52. DOI: 10.1016/j.engstruct.2014.03.017

Toussaint E., Fournely E., Pitti R. M., Grédiac M. [2016]: Studying the mechanical behavior of notched wood beams using full-field measurements. Engineering Structures, 113, 277-286. DOI: 10.1016/j.engstruct.2016.01.052

Vasic S., Smith I., Landis E. [2005]: Finite element techniques and models for wood fracture mechanics. Wood Science and Technology, 39: 3-17. DOI: 10.1007/s00226-004-0255-3

Wang Y., Lee S. H. [2014]: Design and analysis on interference fit in the hardwood dowel-glued joint by finite element method. Procedia Engineering, 79, 166-172. DOI: 10.1016/j.proeng.2014.06.326

Warguła Ł., Wojtkowiak D., Kukla M., Talaśka K. [2020]: Symmetric nature of stress distribution in the elastic-plastic range of Pinus L. pine wood samples determined experimentally and using the finite element method (FEM). Symmetry, 13 [1], 39. DOI: 10.3390/sym13010039

Yörür H. [2012]: Determination of technological properties in simulation (ANSYS) occasion for wooden corner joints. PhD Thesis. Bartın University, Türkiye.

Zhong W., Zhang Z., Chen X., Wei Q., Chen G., Huang X. [2021]: Multi-scale finite element simulation on large deformation behavior of wood under axial and transverse compression conditions. Acta Mechanica Sinica, 37, 1136-1151. DOI:10.1007/s10409-021-01112-z

Zulkifli E., Kusumaningrum P., Rahmi D. P. [2021]: Experimental study and numerical model of spruce and teak wood strength properties under compressive high strain rate loading. Journal of Engineering and Technological Sciences, 53 [1]. DOI: 10.5614/j.eng.technol.sci.2021.53.1.3

List of standards

DIN 52185:1976 Testing of wood; compression test parallel to grain standard by Deutsches Institut Fur Normung E.V. (German National Standard), Germany

DIN 52188:1979 Testing of wood; determination of ultimate tensile stress parallel to grain standard by Deutsches Institut Fur Normung E.V. (German National Standard) Germany

DIN 52192:1979 Testing of wood; compression test perpendicular to grain standard by Deutsches Institut Fur Normung E.V. (German National Standard) Germany

TS 2475:1976 Wood – Determination of Ultimate Tensile Stress Parallel to Grain. Turkish Standards Institution (TSE), Türkiye